JEE Journal of Ecological Engineering

*Journal of Ecological Engineering*, 2026, 27(8), 450–463
https://doi.org/10.12911/22998993/221178
ISSN 2299–8993, License CC-BY 4.0

Received: 2026.04.08
Accepted: 2026.05.27
Published: 2026.07.01

# Performance evaluation of a continuous modular electrocoagulation–filtration system for batik wastewater treatment

Danayanti Azmi Dewi Nusantara[1*], Erina Rahmadyanti[1], Ronny Durrotun Nasihien[2], Dimas Nur Prakoso[3], Sugeng Rifqi Mubaroq[4]

[1] Department of Civil Engineering, Faculty of Engineering, Universitas Negeri Surabaya, Surabaya, Indonesia
[2] Department of Civil Engineering, Faculty of Engineering, Narotama University, Surabaya, Indonesia
[3] Vocational of Electrical Engineering, Madiun State Polytechnic, Madiun, Indonesia
[4] Digital Business, Akademi Digital Bandung, Bandung, Indonesia
* Corresponding author's e-mail: danayantinusantara@unesa.ac.id

## ABSTRACT

Batik wastewater from small-scale industries contains high concentrations of organic matter, suspended solids, and persistent synthetic dyes that pose significant environmental risks if discharged without adequate treatment. This study designed and evaluated the performance of a continuous electrocoagulation–filtration (EC–F) system for treating real batik wastewater under field-representative conditions. The electrocoagulation reactor, constructed from PVC and HDPE, was equipped with ten iron plate electrodes (mild steel, 30 × 50 cm, total active anode area 7500 $cm^2$) arranged at inter-electrode distances of 2 and 4 cm, operated at current densities of 8–18 $mA/cm^2$. A downstream multi-media filtration unit (silica sand, activated carbon, zeolite) served as a polishing stage. The system was operated at detention times of 50, 75, and 100 minutes. Under optimal conditions (2 cm spacing, 100 min, 18 $mA/cm^2$), the integrated system achieved removal efficiencies of 95.4% for COD, 94.4% for BOD, 98.3% for TSS, and 99.0% for color, with an energy consumption of 3.1 $kWh/m^3$ and an estimated operational cost of USD 0.64/$m^3$. Two-way ANOVA confirmed that both electrode spacing and detention time significantly influenced pollutant removal ($p < 0.001$), with synergistic interaction effects for COD and TSS. The treated effluent complied with Indonesian Ministry of Environment Regulation No. 5/2014. These results demonstrate that the continuous EC–F system is a practical, scalable, and cost-effective decentralized treatment solution for small-scale batik industries.

**Keywords:** batik wastewater, electrocoagulation-filtration, continuous treatment system, iron electrodes, small-scale industries, energy consumption.

## INTRODUCTION

The batik industry is a key component of Indonesia's creative economy, serving as a driver of cultural preservation and economic growth (Gunawan et al., 2022). As a prominent product of small and medium enterprises (SMEs), batik represents national heritage and is exported to countries including the United States, Canada, Australia, Singapore, and Spain. In 2020, batik exports reached approximately 21.5 million US dollars, underscoring its economic significance (Raya et al., 2021).

Despite its economic importance, batik production generates substantial volumes of wastewater, particularly during the dyeing and wax-removal (lorod) stages, which involve the intensive use of synthetic dyes and chemical auxiliaries (Zakaria et al., 2023). The resulting wastewater typically contains elevated levels of chemical oxygen demand (COD), biological oxygen demand (BOD), synthetic dyes, and potentially heavy metals, all of which pose environmental hazards if discharged without proper treatment (Tangahu et al., 2019). Many small-scale batik enterprises operate in areas lacking centralized wastewater

treatment infrastructure, leading to the discharge of untreated or inadequately treated effluent into water bodies (Kusumawardani et al., 2024). The chemical stability and bio-recalcitrance of synthetic dye compounds hinder their natural degradation, threatening aquatic ecosystems and public health (Rahmadyanti and Febriyanti, 2020; Rahmadyanti and Wiyono, 2020). Consequently, there is an urgent need for effective and accessible wastewater treatment solutions for these industries (Triwiswara, 2019).

Conventional treatment methods, including chemical coagulation, biological processes, and advanced oxidation, often face limitations such as high energy requirements, operational complexity, and insufficient removal of persistent pollutants. These technologies frequently require substantial infrastructure and specialized expertise, making them impractical for small-scale operations (Worku et al., 2025). Moreover, individual treatment processes are often inadequate for the complex composition of textile wastewater, prompting growing interest in integrated treatment approaches (Bidu et al., 2021).

Electrocoagulation (EC) has emerged as a promising alternative owing to its compact footprint, in situ coagulant generation, minimal chemical requirements, reduced sludge production, and operational simplicity (Bhagawati et al., 2022). These characteristics make EC particularly suitable for decentralized and small-scale applications. However, the majority of EC studies on batik and textile wastewater have been conducted in batch mode (Reza et al., 2024; Fadzli et al., 2024). Batch systems are prone to performance inconsistency, require extensive manual intervention, and are poorly suited for continuous industrial effluent treatment, limiting their long-term applicability.

Recent advances in environmental engineering have emphasized the use of continuous-flow integrated systems to improve operational consistency, treatment effectiveness, and scalability. Coupling EC with downstream filtration has been shown to enhance effluent quality by capturing residual flocs and suspended particles (Kuokkanen et al., 2021; Aryanti et al., 2022). Nevertheless, comprehensive evaluations of continuous EC–filtration (EC–F) systems using real batik wastewater under field-representative conditions remain scarce. Most existing studies rely on synthetic wastewater, laboratory-scale batch configurations, or isolated unit processes, which do not adequately reflect the performance of integrated systems in real-world small industry settings (Salinas-Echeverria et al., 2023; Lamhar et al., 2024).

This study addresses this gap by presenting the design and performance evaluation of a modular continuous EC–F system specifically developed for treating real batik wastewater from small-scale operations. Unlike previous studies that predominantly employed batch reactors or synthetic effluents, this work integrates a dual-stage iron electrode EC unit with a multi-media filtration unit operating under continuous flow, enabling more consistent treatment performance under varying influent conditions. The effects of inter-electrode spacing and hydraulic detention time on pollutant removal efficiency were systematically investigated using two-way ANOVA with interaction analysis. This approach provides insights into both the underlying treatment mechanisms and practical design considerations for decentralized wastewater treatment in small and medium batik enterprises.

## MATERIAL AND METHODS

### Batik wastewater characterization

Wastewater samples were collected from a local batik workshop located in Sidomukti Village, Magetan Regency, East Java, Indonesia. Samples were obtained at the wax-removal (lorod) stage, immediately after boiling and dye fixation, as this stage produces wastewater with the highest concentrations of organic matter and chemical residues compared to washing or dyeing stages (Rahmadyanti and Audina, 2020).

The collected samples were analyzed immediately without preservation to maintain their original characteristics. The following water quality parameters were measured: COD by the closed reflux dichromate method according to SNI 6989.2:2009 (Aryanti et al., 2022; Asaithambi et al., 2024), TSS by the gravimetric filtration method according to SNI 6989.3:2019, and BOD by the Winkler method (Aryanti et al., 2022; Bagastyo et al., 2023).

The initial wastewater characterization revealed high pollutant concentrations: COD of 1200 mg/L, BOD of 450 mg/L, TSS of 1200 mg/L, and color intensity of 2000 Pt-Co. The influent pH was 9.2, electrical conductivity was 2150 uS/cm, and the wastewater temperature at

the time of analysis was 30 +/- 2 °C. These elevated levels are attributed to the use of various sodium-based compounds (sodium salts, sodium alginate, and sodium silicate) and synthetic dyes commonly employed in batik processing (Phang et al., 2022; Xie et al., 2024). The high conductivity reflects the substantial dissolved ionic content originating from sodium-based auxiliaries, which also facilitates electrical current flow during the EC process. According to Indonesian Ministry of Environment Regulation No. 5 of 2014, the maximum permissible discharge limits for COD, BOD, and TSS are 125 mg/L, 45 mg/L, and 40 mg/L, respectively. The initial concentrations substantially exceeded these limits, confirming the need for effective treatment prior to discharge. Table 1 summarizes the initial wastewater characteristics.

## System design and configuration

The EC–F treatment system was designed as a modular sequential reactor with a total treatment capacity of 1 $m^3$. The system comprised the following components: an equalization tank, an inlet chamber, two EC chambers, an intermediate chamber, an intermediate tank, a filtration unit, and a sampling tank. The equalization, intermediate, and sampling tanks were constructed from high-density polyethylene (HDPE) with a capacity of 150 L each. The EC chambers were fabricated from polyvinyl chloride (PVC) and equipped with iron (Fe) plate electrodes. Iron electrodes were selected for their capacity to generate iron-based coagulant species in situ, enabling effective removal of organic compounds and suspended solids at relatively low material cost (Rakhmania et al., 2022; Hellal et al., 2023).

Each EC chamber measured 0.44 × 0.6 × 1.2 m and was equipped with 10 iron plate electrodes (5 anodes + 5 cathodes) arranged in a monopolar parallel configuration. The electrode plates were fabricated from low-carbon mild steel (equivalent to JIS SS400 / ASTM A36), with dimensions of 30 × 50 cm and a thickness of 3 mm. The total effective anode surface area was 7500 $cm^2$ per chamber (5 anode plates × 30 × 50 cm). The inter-electrode distances tested were 2 cm and 4 cm. The applied current density varied depending on the electrode spacing and detention time, ranging from 8 to 18 $mA/cm^2$, with corresponding applied voltages of 13.8–24.0 V (Table 2).

It should be noted that in this experimental design, current density co-varied with electrode spacing and detention time, as the power supply delivered different currents depending on the cell resistance (which changes with electrode gap) and operational adjustments at each detention time. Consequently, the individual effects of these three parameters cannot be fully disentangled, and

**Table 1.** Characteristics of raw batik wastewater

| Parameter | Unit | Value | Discharge limit (Reg. No. 5/2014) |
|---|---|---|---|
| COD | mg/L | 1200 | 125 |
| BOD | mg/L | 450 | 45 |
| TSS | mg/L | 1200 | 40 |
| Color | Pt-Co | 2000 | – |
| pH | – | 9.2 | 6.0–9.0 |
| Conductivity | uS/cm | 2150 | – |
| Temperature | °C | 30 +/- 2 | – |
| $BOD_5$ | Between groups | | |

**Table 2.** Operating conditions for each experimental configuration

| Electrode spacing | Detention time (min) | Current density ($mA/cm^2$) | Applied voltage (V) | Energy consumption ($kWh/m^3$) |
|---|---|---|---|---|
| 4 cm | 50 | 8 | 24.0 | 1.2 |
| 4 cm | 75 | 10 | 19.2 | 1.8 |
| 4 cm | 100 | 12 | 16.0 | 2.4 |
| 2 cm | 50 | 12 | 21.3 | 1.6 |
| 2 cm | 75 | 15 | 16.4 | 2.3 |
| 2 cm | 100 | 18 | 13.8 | 3.1 |

the results should be interpreted as reflecting the combined influence of the operating conditions.

Wastewater transfer between units was facilitated by three pumps: a submersible pump (80 L/min) for initial flow, a filtration pump (38 L/min) for transfer from the intermediate tank to the filtration unit, and a sampling pump (80 L/min) for delivery to the sampling tank. The system was operated using an electrical control panel with 220 V supply voltage and 16 A current capacity to maintain stable treatment conditions.

The downstream filtration unit served as a polishing stage and consisted of two vertical columns (0.14 $m^3$ each, base area approximately 35 × 40 cm, effective height 100 cm). Each column was packed with three layers of filter media (from top to bottom): zeolite (25 cm, particle size 2.0–4.0 mm), granular activated carbon (35 cm, particle size 1.0–2.0 mm), and silica sand (30 cm, particle size 0.5–1.0 mm), supported by a 10 cm gravel layer (5–10 mm) at the base. This multimedia configuration was designed to remove residual suspended solids, dissolved organic compounds, and remaining metal species after the EC process (Channa et al., 2024; Bakry et al., 2024).

Figure 1 illustrates the schematic configuration and photographs of the EC–F system. The schematic diagram (Figure 1a) shows the sequential arrangement of treatment units from the equalization tank through the EC chambers with baffle channel floculator, sedimentation, filtration (quartz sand and activated carbon), and the effluent tank. Photographs of the actual system (Figure 1b) show: (i) the electrical control panel and assembled EC unit; (ii) the equalization tank during wastewater homogenization; (iii) the EC chamber with vertically arranged parallel iron plate electrodes; (iv) raw batik wastewater (dark-colored, high turbidity); and (v) treated effluent (clear, low turbidity), visually demonstrating the treatment effectiveness.

## Experimental procedure

The treatment process began in the equalization tank, which served to store and homogenize the wastewater, stabilizing pollutant concentrations prior to the main treatment stage. From the equalization tank, wastewater was automatically transferred to the inlet chamber and subsequently passed through the primary EC chamber, the intermediate chamber, and the secondary EC chamber, with detention times of 50, 75, and 100 minutes. Pump operation was regulated by a float switch that activated the submersible pump when the water level reached a predetermined height, ensuring consistent flow between units without manual intervention (Bhagawati et al., 2022).

After passing through both EC stages, the treated effluent flowed into the intermediate tank, then through the filtration unit, and finally into the sampling tank. Samples for laboratory analysis were collected from the sampling tank upon completion of all treatment stages. The parameters analyzed were COD, BOD, and TSS, which are widely recognized as key indicators of textile industrial wastewater pollution (Wang et al., 2022; Islam et al., 2025).

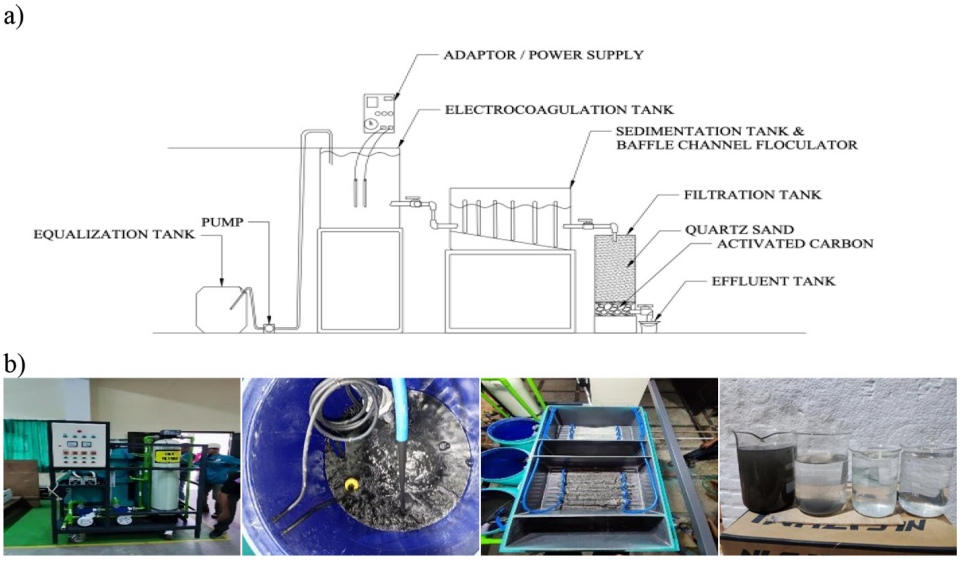


**Figure 1.** (a) Schematic diagram of the continuous EC–F system; (b) photographs of the system components and visual comparison of raw and treated batik wastewater

Analytical methods were as follows: COD was determined by the closed reflux dichromate method (SNI 06-6989.2:2009) (Aziz et al., 2016); TSS was measured by gravimetric filtration (SNI 6989.3:2019) using pre-weighed filter media (Ghaderi and Rahbani, 2021); and BOD was measured by the Winkler method (Susilowati et al., 2018). The use of standardized analytical methods ensured accuracy and comparability of results (Kholisoh et al., 2022).

Experiments were conducted at inter-electrode distances of 2 cm and 4 cm, yielding a total of six treatment conditions (2 electrode spacings × 3 detention times). Each treatment condition was performed in triplicate using independent experimental runs with fresh batik wastewater batches, resulting in 18 total experimental runs. This approach was adopted to ensure data reliability and account for the inherent variability of real industrial wastewater characteristics (Hashem et al., 2024).

For each experimental run, the system was operated continuously until steady-state conditions were achieved, defined as the point at which effluent quality parameters stabilized – typically after a minimum of one hydraulic detention time of continuous operation. Effluent samples were collected only after steady-state was confirmed. All experiments were carried out under ambient temperature (30 +/- 2 °C) and the natural pH of the wastewater (pH 9.2) to simulate realistic operating conditions in small-scale batik industries.

Removal efficiencies were calculated based on the concentration difference between influent and effluent samples, as presented in Equation 1:

$$Removal\ efficiency\ (\%) = \left[\frac{C_{influent} - C_{effluent}}{C_{influent}}\right] \times 100 \quad (1)$$

### Statistical analysis

One-way analysis of variance (ANOVA) was performed to evaluate the statistical significance of differences in pollutant removal efficiency among the six treatment conditions at a 95% confidence level (alpha = 0.05). Two-way ANOVA was subsequently performed to assess the individual and interaction effects of electrode spacing and detention time on removal efficiency. When ANOVA indicated statistically significant differences, Tukey's honestly significant difference (HSD) post hoc test was conducted to identify specific pairwise differences among treatment groups. Pearson correlation analysis was used to examine relationships among operational and performance parameters. All statistical analyses were performed using Python (SciPy v1.11, statsmodels v0.14). The treated effluent quality was also compared against the textile industrial wastewater discharge standards stipulated in Indonesian Ministry of Environment Regulation No. 5 of 2014 (Kholisoh et al., 2022).

## RESULTS AND DISCUSSION

### Treatment performance of the EC–F system

Table 3 summarizes the pollutant removal performance of the continuous EC–F system under all tested conditions. Across all parameters, smaller inter-electrode spacing (2 cm) and longer detention time (100 min) consistently yielded the highest removal efficiencies.

The EC–F system achieved substantial COD reductions across all tested conditions (Figure 2). At an inter-electrode distance of 4 cm, removal efficiencies ranged from 55.6% (50 min) to 77.5% (100 min). Reducing the electrode spacing to 2 cm improved COD removal to 67.5–95.4%, with the maximum efficiency achieved at 100 min detention time. BOD removal followed a similar trend (Figure 3), ranging from 40.0% to 94.4% across all conditions. TSS removal (Figure 4) ranged from 44.2% to 98.3%, with the largest absolute reductions observed at 2 cm spacing due to the high initial TSS concentration (1200 mg/L).

The EC–F system also demonstrated excellent color removal (Table 4). The initial dark-colored wastewater (2000 Pt-Co) was substantially decolorized under all conditions, achieving 75.0–99.0% removal. At optimal conditions (2 cm, 100 min), near-complete decolorization (99.0%, residual 20 Pt-Co) was observed, indicating effective destabilization and removal of chromophoric dye molecules through iron hydroxide floc adsorption and co-precipitation. The influent pH of 9.2 decreased progressively with increasing current density, with effluent pH values ranging from 7.2 to 8.5 – all within the acceptable regulatory range of 6.0–9.0. The pH reduction is attributed to hydroxide ion consumption during iron hydroxide formation and hydrogen gas generation at the cathode. Sludge production ranged from 0.8 to 2.3 g/L, increasing with current density and detention time, consistent with Faraday's law governing electrode dissolution.

**Table 3.** Summary of effluent concentrations (mean +/- SD, n = 3), removal efficiencies, and regulatory compliance

| Parameter | Initial (mg/L) | Spacing | Time (min) | Effluent (mg/L) | SD | Removal (%) | Limit (mg/L) | Compliance |
|---|---|---|---|---|---|---|---|---|
| COD | 1.200 | 4 cm | 50 | 533.3 | +/-12.6 | 55.6 | 125 | No |
| COD | 1.200 | 4 cm | 75 | 413.3 | +/-15.3 | 65.6 | 125 | No |
| COD | 1.200 | 4 cm | 100 | 270.0 | +/-10.0 | 77.5 | 125 | No |
| COD | 1.200 | 2 cm | 50 | 390.0 | +/-10.0 | 67.5 | 125 | No |
| COD | 1.200 | 2 cm | 75 | 250.0 | +/-10.0 | 79.2 | 125 | No |
| COD | 1.200 | 2 cm | 100 | 55.0 | +/-5.0 | 95.4 | 125 | **Yes** |
| BOD | 450 | 4 cm | 50 | 270.0 | +/-10.0 | 40.0 | 45 | No |
| BOD | 450 | 4 cm | 75 | 210.0 | +/-10.0 | 53.3 | 45 | No |
| BOD | 450 | 4 cm | 100 | 130.0 | +/-10.0 | 71.1 | 45 | No |
| BOD | 450 | 2 cm | 50 | 190.0 | +/-10.0 | 57.8 | 45 | No |
| BOD | 450 | 2 cm | 75 | 120.0 | +/-10.0 | 73.3 | 45 | No |
| BOD | 450 | 2 cm | 100 | 25.0 | +/-5.0 | 94.4 | 45 | **Yes** |
| TSS | 1200 | 4 cm | 50 | 670.0 | +/-20.0 | 44.2 | 40 | No |
| TSS | 1200 | 4 cm | 75 | 540.0 | +/-20.0 | 55.0 | 40 | No |
| TSS | 1200 | 4 cm | 100 | 320.0 | +/-20.0 | 73.3 | 40 | No |
| TSS | 1200 | 2 cm | 50 | 420.0 | +/-20.0 | 65.0 | 40 | No |
| TSS | 1200 | 2 cm | 75 | 220.0 | +/-20.0 | 81.7 | 40 | No |
| TSS | 1200 | 2 cm | 100 | 20.0 | +/-5.0 | 98.3 | 40 | **Yes** |

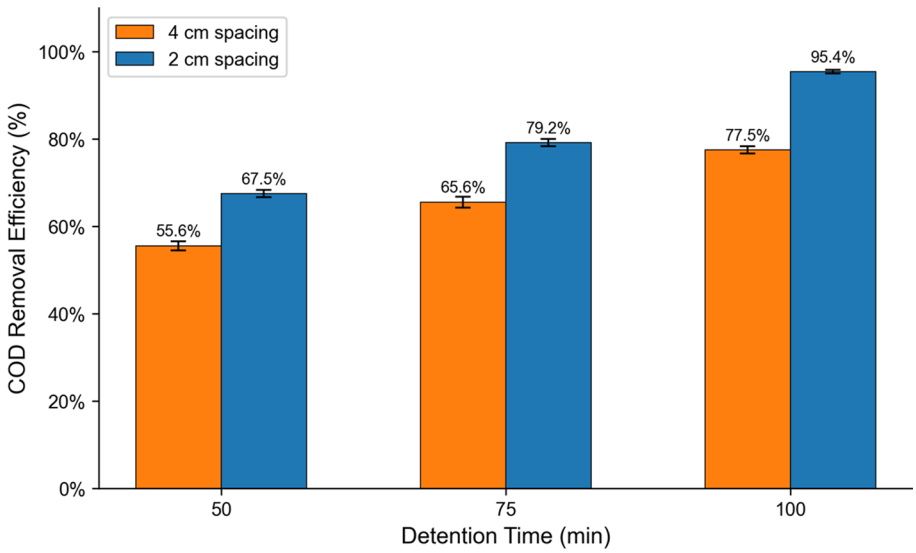


**Figure 2.** Effect of inter-electrode spacing and detention time on COD removal efficiency. Error bars represent +/- SD (n = 3)

**Table 4.** Color removal, pH, energy consumption, and sludge production under different operating conditions

| Spacing | Time (min) | CD ($mA/cm^2$) | Color influent (Pt-Co) | Color effluent (Pt-Co) | Color removal (%) | pH effluent | Energy ($kWh/m^3$) | Sludge (g/L) |
|---|---|---|---|---|---|---|---|---|
| 4 cm | 50 | 8 | 2000 | 500 | 75.0 | 8.5 | 1.2 | 0.8 |
| 4 cm | 75 | 10 | 2000 | 300 | 85.0 | 8.1 | 1.8 | 1.2 |
| 4 cm | 100 | 12 | 2000 | 160 | 92.0 | 7.8 | 2.4 | 1.5 |
| 2 cm | 50 | 12 | 2000 | 240 | 88.0 | 8.0 | 1.6 | 1.2 |
| 2 cm | 75 | 15 | 2000 | 100 | 95.0 | 7.6 | 2.3 | 1.8 |
| 2 cm | 100 | 18 | 2000 | 20 | 99.0 | 7.2 | 3.1 | 2.3 |

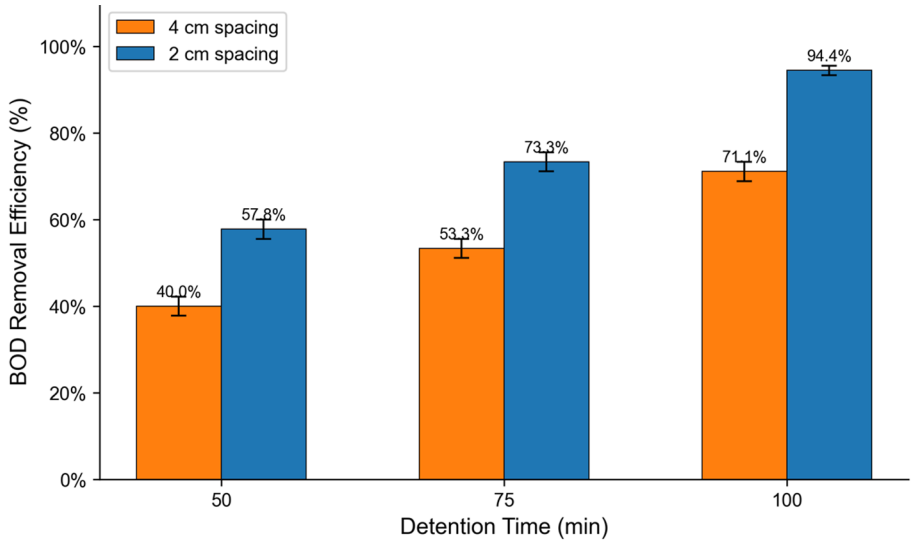


**Figure 3.** Effect of inter-electrode spacing and detention time on BOD removal efficiency. Error bars represent +/- SD (n = 3)

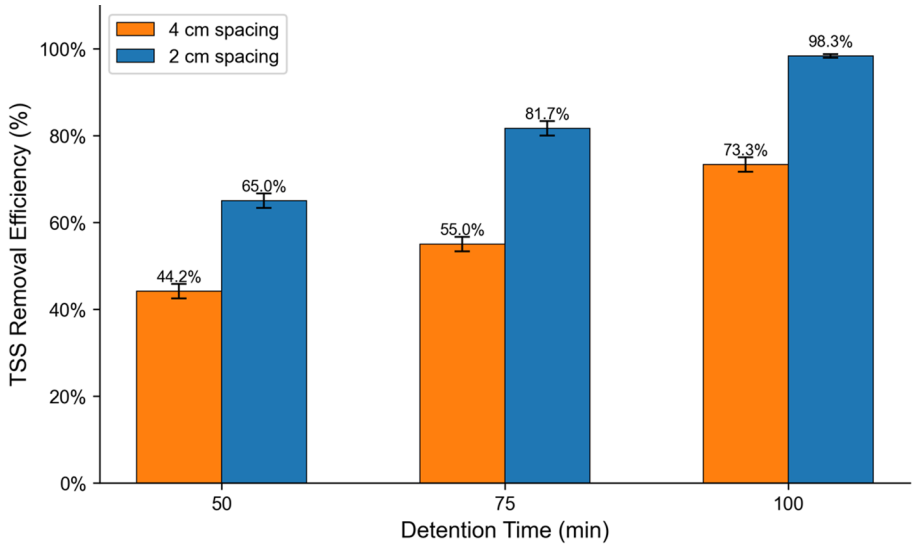


**Figure 4.** Effect of inter-electrode spacing and detention time on TSS removal efficiency. Error bars represent +/- SD (n = 3)

## Statistical analysis of operational parameters

One-way ANOVA confirmed highly significant differences in removal efficiency among the six treatment conditions for all parameters (Table 5). Two-way ANOVA (Table 6) was subsequently performed to disentangle the effects of electrode spacing and detention time.

Both electrode spacing and detention time were highly significant factors for all three parameters ($p < 0.001$). Notably, two-way ANOVA revealed significant synergistic interaction effects for COD ($F = 17.17$, $p < 0.001$) and TSS ($F = 5.78$, $p = 0.017$), indicating that the combined effect of smaller spacing and longer detention time exceeded the sum of their individual contributions. For BOD, the interaction was not significant ($p = 0.107$), suggesting additive rather than synergistic effects. It should be noted, however, that the co-variation of current density with electrode spacing and detention time means that these interaction effects reflect the combined influence of all three parameters rather than spacing and time alone.

Tukey's HSD post hoc test (Table 7) confirmed that the optimal condition (2 cm, 100 min) was statistically distinguishable from all other conditions for all parameters ($p < 0.001$). Some intermediate conditions showed overlapping performance; for instance, COD removal at 2 cm/50 min and 4 cm/75 min were not statistically

**Table 5.** One-way ANOVA results for pollutant removal efficiency across treatment conditions

| Parameter | Source | df | SS | MS | F-value | p-value |
|---|---|---|---|---|---|---|
| COD | Between groups | 5 | 2848.66 | 569.73 | 686.86 | <0.001 |
| COD | Residual | 12 | 9.95 | 0.83 | – | – |
| BOD | Between groups | 5 | 5361.11 | 1072.22 | 248.14 | <0.001 |
| BOD | Residual | 12 | 51.85 | 4.32 | – | – |
| TSS | Between groups | 5 | 5598.96 | 1119.79 | 477.78 | <0.001 |
| TSS | Residual | 12 | 28.13 | 2.34 | – | – |

**Table 6.** Two-way ANOVA results (spacing x detention time interaction)

| Parameter | Source | df | SS | MS | F-value | p-value | Significant |
|---|---|---|---|---|---|---|---|
| COD | Spacing | 1 | 944.92 | 944.92 | 1139.17 | <0.001 | Yes |
| COD | Time | 2 | 1875.25 | 937.63 | 1130.38 | <0.001 | Yes |
| COD | Spacing × Time | 2 | 28.49 | 14.25 | 17.17 | <0.001 | Yes |
| COD | Residual | 12 | 9.95 | 0.83 | – | – | – |
| BOD | Spacing | 1 | 1867.28 | 1867.28 | 432.14 | <0.001 | Yes |
| BOD | Time | 2 | 3470.37 | 1735.19 | 401.57 | <0.001 | Yes |
| BOD | Spacing × Time | 2 | 23.46 | 11.73 | 2.71 | 0.107 | No |
| BOD | Residual | 12 | 51.85 | 4.32 | – | – | – |
| TSS | Spacing | 1 | 2628.13 | 2628.13 | 1121.33 | <0.001 | Yes |
| TSS | Time | 2 | 2943.75 | 1471.88 | 628.00 | <0.001 | Yes |
| TSS | Spacing × Time | 2 | 27.08 | 13.54 | 5.78 | 0.017 | Yes |
| TSS | Residual | 12 | 28.13 | 2.34 | – | – | – |

**Table 7.** Tukey HSD post hoc pairwise comparisons (selected)

| Parameter | Comparison | Mean diff (%) | 95% CI | p-adj | Significant |
|---|---|---|---|---|---|
| COD | 2 cm/100 vs 4 cm/50 | 39.86 | [37.36, 42.36] | <0.001 | Yes |
| COD | 2 cm/100 vs 4 cm/100 | 17.92 | [15.42, 20.41] | <0.001 | Yes |
| COD | 2 cm/100 vs 2 cm/75 | 16.25 | [13.75, 18.75] | <0.001 | Yes |
| COD | 2 cm/50 vs 4 cm/75 | 1.94 | [-0.55, 4.44] | 0.167 | No |
| BOD | 2 cm/100 vs 4 cm/50 | 54.44 | [48.74, 60.15] | <0.001 | Yes |
| BOD | 2 cm/100 vs 2 cm/75 | 21.11 | [15.41, 26.81] | <0.001 | Yes |
| BOD | 2 cm/75 vs 4 cm/100 | 2.22 | [-3.48, 7.92] | 0.775 | No |
| TSS | 2 cm/100 vs 4 cm/50 | 54.17 | [49.97, 58.37] | <0.001 | Yes |
| TSS | 2 cm/100 vs 2 cm/75 | 16.67 | [12.47, 20.87] | <0.001 | Yes |

**Note:** Only selected pairwise comparisons are shown. Full results are available in Supplementary Table S1.

different (p = 0.167), suggesting that similar removal efficiency can be achieved through different combinations of spacing and time.

## Mechanisms of pollutant removal

The removal of COD, BOD, and TSS in the EC process is governed by a common electrochemical mechanism. When an electrical current is applied, the iron anode undergoes oxidative dissolution, releasing $Fe_2^+$ and $Fe_3^+$ ions into solution:

$$Anode: Fe \rightarrow Fe^{2+} + 2e^- \quad (2)$$

$$Cathode: 2H_2O + 2e^- \rightarrow H_2 \uparrow + 2OH^- \quad (3)$$

$$Hydrolysis: Fe^{2+}/Fe^{3+} + nOH^- \rightarrow Fe(OH)_n \quad (4)$$

The resulting iron hydroxide species – primarily $Fe(OH)_2$ and $Fe(OH)_3$ – possess high surface

area and strong adsorption capacity. These species function as effective coagulants through two principal mechanisms: (i) charge neutralization, whereby the positively charged iron hydroxides destabilize negatively charged colloidal particles and suspended solids, promoting aggregation into larger, settleable flocs; and (ii) sweep flocculation, in which the precipitating iron hydroxides enmesh dissolved and colloidal organic compounds during floc formation (Jing et al., 2020; Al-Shati et al., 2023; Tegladza et al., 2021).

For COD removal, the iron hydroxide flocs adsorb dissolved organic compounds – including aromatic dye molecules and their auxiliary chemicals – that contribute to the chemical oxygen demand (Tabash et al., 2024; Sadaf et al., 2024). For BOD removal, the coagulation process captures biodegradable organic substrates, reducing their availability for microbial degradation (Bener et al., 2019; De Maman et al., 2022; Fan et al., 2023). For TSS removal, charge neutralization of fine suspended and colloidal particles causes destabilization, aggregation, and subsequent separation by sedimentation (Shah et al., 2024; Ahmed et al., 2024; Abfertiawan et al., 2024).

Reducing the electrode spacing from 4 cm to 2 cm consistently improved removal efficiency, attributable to the increased electric field intensity and accelerated Fe anode dissolution at smaller electrode gaps (Almukdad et al., 2021; Phu et al., 2025). Increasing the detention time from 50 to 100 minutes also progressively improved removal, due to extended electrochemical reactions and more complete floc maturation.

The integration of EC with a downstream multi-media filtration unit further enhanced treatment performance. The filtration stage effectively retained residual iron hydroxide flocs and adsorbed organic compounds formed during EC, preventing pollutant carry-over into the final effluent (Al-Shati et al., 2023; Ardianto et al., 2025; Al-Qodah et al., 2025; Behera et al., 2025). It should be noted that the reported removal efficiencies represent the combined performance of the integrated EC–F system; the individual contributions of the EC and filtration stages were not separately quantified in this study, which represents a limitation.

## Energy efficiency, correlation analysis, and practical implications

Energy consumption ranged from 1.2 kWh/m$^3$ (4 cm, 50 min) to 3.1 kWh/m$^3$ (2 cm, 100 min), as shown in Table 4. At optimal conditions, the system consumed 3.1 kWh/m$^3$ while achieving removal efficiencies exceeding 94% for all parameters. This energy requirement is competitive with values reported for EC treatment of textile wastewater, which typically range from 1.0 to 10.0 kWh/m$^3$ (Gasmi et al., 2022; Manikandan and Saraswathi, 2023). However, energy efficiency analysis revealed diminishing returns at longer detention times: COD removal per unit energy decreased from 46.3%/(kWh/m$^3$) at 4 cm/50 min to 30.8%/(kWh/m$^3$) at 2 cm/100 min (Reategui-Romero et al., 2020).

Pearson correlation analysis (n = 6 operating conditions) revealed strong positive associations between current density and pollutant removal: COD ($r = 0.962$, $p = 0.002$), BOD ($r = 0.965$, $p = 0.002$), and TSS ($r = 0.986$, $p < 0.001$). Energy consumption was also strongly correlated with removal efficiency ($r = 0.985$, $p < 0.001$ for COD) and sludge production ($r = 0.968$, $p = 0.002$), consistent with Faraday's law. Effluent pH showed strong negative correlations with all removal parameters ($r = -0.98$ to $-0.99$). While these correlations are statistically significant, the small sample size (n = 6) warrants cautious interpretation; validation with additional operating conditions would strengthen these findings (Figure 5).

## Comparative performance, cost analysis, and regulatory compliance

The optimal operating conditions (2 cm electrode spacing, 100 min detention time, 18 mA/cm$^2$) produced effluent concentrations of 55.0 mg/L (COD), 25.0 mg/L (BOD), 20.0 mg/L (TSS), and 20 Pt-Co (color), with an effluent pH of 7.2. All parameters comply with the discharge limits specified in Indonesian Ministry of Environment Regulation No. 5 of 2014 (COD <= 125 mg/L, BOD <= 45 mg/L, TSS <= 40 mg/L, pH 6.0–9.0).

Table 8 presents a comparison with previously reported EC systems. The EC–F system achieved the highest COD removal (95.4%) among the compared studies while maintaining competitive energy consumption (3.1 kWh/m$^3$).

The operational cost was estimated based on energy consumption and electrode material costs (Table 9). Using the Indonesian industrial electricity tariff of IDR 1035.78/kWh (PLN tariff for industrial category I-1/I-2, Q4 2025) and an estimated iron plate cost of IDR 15,000/kg, the operational cost at optimal conditions was IDR 10,261/m$^3$ (approximately USD 0.64/m$^3$).

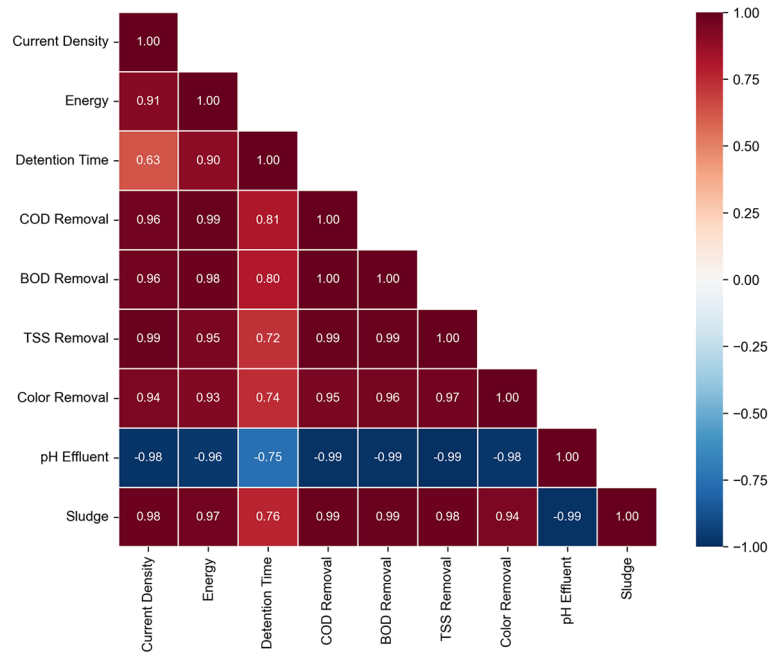


**Figure 5.** Correlation heatmap of treatment parameters (n = 6 operating conditions)

**Table 8.** Comparison of treatment performance with previous EC studies

| Reference | Wastewater | Mode | Electrode | COD removal (%) | Energy (kWh/m³) | Cost (USD/m³) |
|---|---|---|---|---|---|---|
| Bener et al. (2019) | Real textile | Batch | Fe | 18.6 (COD); 65% TOC | N/R | 1.50 |
| De Maman et al. (2022) | Real textile | Batch | Fe slag | 55 | N/R | N/R |
| Al-Shati et al. (2023) | High-strength organic | Batch | Fe | 85–91 | 3.2–5.1 | N/R |
| Fadzli et al. (2024) | Batik (real + simulated) | Batch | Al/Fe | 60–85 | N/R | N/R |
| Lamhar et al. (2024) | Synthetic textile | Continuous | Al | 70–90 (color) | 2.0–6.5 | N/R |
| Hashem et al. (2024) | Real + synthetic | Batch | Fe/Al | 70–88 | 1.5–4.5 | N/R |
| This study | Real batik | Continuous EC–F | Fe | 95.4 | 1.2–3.1 | 0.17–0.64 |

**Note:** N/R – not reported.

**Table 9.** Estimated operational cost of the EC–F system

| Spacing | Time (min) | Energy cost (IDR/m³) | Electrode cost (IDR/m³) | Total (IDR/m³) | Total (USD/m³) |
|---|---|---|---|---|---|
| 4 cm | 50 | 1243 | 1500 | 2743 | 0.17 |
| 4 cm | 75 | 1864 | 3000 | 4864 | 0.30 |
| 4 cm | 100 | 2486 | 4650 | 7136 | 0.45 |
| 2 cm | 50 | 1657 | 2400 | 4057 | 0.25 |
| 2 cm | 75 | 2382 | 4350 | 6732 | 0.42 |
| 2 cm | 100 | 3211 | 7050 | 10,261 | 0.64 |

**Note:** USD conversion at IDR 16,000/USD. Electrode consumption estimated using Faraday's law. Costs exclude filter media replacement, labor, and maintenance.

This cost is competitive with the reported range of USD 0.25–4.93/m³ for EC treatment of various wastewaters. For a typical small-scale batik enterprise generating 1–3 m³ of wastewater per day, this translates to a daily treatment cost of approximately IDR 10,000–31,000 (USD 0.64–1.92/day), which is economically feasible for SME operations.

The EC–F system demonstrated several practical advantages for decentralized application: (i) compact modular design suitable for space-constrained workshops; (ii) in situ coagulant generation eliminating chemical procurement; (iii) relatively low sludge production (0.8–2.3 g/L); (iv) moderate energy requirements (1.2–3.1 kWh/m³); and (v)

straightforward operation requiring minimal technical expertise (Al Jaberi et al., 2023; Sadaf et al., 2024; Issaka et al., 2024; Garcia-Avila et al., 2025).

### Limitations and future research

Several limitations of this study should be acknowledged. First, current density co-varied with electrode spacing and detention time, precluding independent assessment of each parameter's effect. Future studies should employ a full factorial design with independent current density control. Second, the individual contributions of the EC and filtration stages were not separately quantified; intermediate sampling between EC and filtration units would clarify each stage's contribution. Third, the kinetic and correlation analyses were limited by the small number of operating conditions (n = 6) and time points (n = 3), which restricts the robustness of kinetic modeling and correlation inference. Fourth, long-term operational stability, electrode passivation, and filter media exhaustion were not assessed. Future research should address: (i) extended operation trials over weeks to months; (ii) integration with renewable energy sources; (iii) sludge characterization and disposal strategies; and (iv) pilot-scale validation across batik production sites with varying wastewater characteristics.

## CONCLUSIONS

This study demonstrated that a continuous EC-F system can effectively treat actual batik wastewater under field-representative conditions. The key findings are as follows:

1. The integrated dual-stage iron EC and multimedia filtration process achieved maximum removal efficiencies of 95.4% for COD, 94.4% for BOD, 98.3% for TSS, and 99.0% for color at optimal conditions (2 cm electrode spacing, 100 min detention time, 18 mA/cm$^2$), with an energy consumption of 3.1 kWh/m$^3$ and an estimated operational cost of USD 0.64/m$^3$.
2. Two-way ANOVA confirmed that both electrode spacing and detention time significantly influenced pollutant removal ($p < 0.001$), with synergistic interaction effects for COD ($p < 0.001$) and TSS ($p = 0.017$).
3. Pearson correlation analysis revealed strong associations ($r > 0.96$) between current density and all pollutant removal efficiencies, supporting the role of enhanced coagulant generation as the primary performance driver.
4. Under optimal conditions, the treated effluent met all discharge limits specified in Indonesian Ministry of Environment Regulation No. 5 of 2014.
5. The system's compact design, operational simplicity, moderate energy requirements, and low operational costs make it suitable for decentralized application in small and medium batik enterprises.

### Acknowledgements

This research was financially supported by the Ministry of Higher Education, Science, and Technology of the Republic of Indonesia under the Applied Research Grant Scheme for Prototype-Based Product Outputs (Fiscal Year 2025), contract number 090/C3/DT.05.00/PL/2025, dated May 28, 2025. The authors gratefully acknowledge this financial support.

## REFERENCES

1. Abfertiawan, M.S., Syafila, M., Handajani, M., Hasan, F., Oktaviani, H., Gunawan, F. and Djali, F. (2024) Batch electrocoagulation process for the removal of high colloidal clay from open-cast coal mine water using Al and Fe electrodes. Mine Water and The Environment, 43, 516–528. https://doi.org/10.1007/s10230-024-01004-1
2. Ahmed, T., Ahsan, A., Khan, M.H.R.B., Nahian, T.K., Antar, R.H., Hasan, A., Karim, M.R., Shafiquzzaman, M. and Imteaz, M. (2024). Comprehensive study on the selection and performance of the best electrode pair for electrocoagulation of textile wastewater using multi-criteria decision-making methods (TOPSIS, VIKOR and PROMETHEE II). Journal of Environmental Management, 363, 121337. https://doi.org/10.1016/j.jenvman.2024.121337
3. Al Jaberi, F.Y., Alardhi, S.M., Ahmed, S.A., Salman, A.D., Juzsakova, T., Cretescu, I., Le, P-C., Chung, W.J., Chang, S.W. and Nguyen, D.D. (2022). Can electrocoagulation technology be integrated with wastewater treatment systems to improve treatment efficiency? Environmental Research, 214, 2, 113890. https://doi.org/10.1016/j.envres.2022.113890
4. Al Jaberi, F.Y., Ahmed, S.A., Makki, H.F., Naje, A.S., Zwain, H.M., Salman, A.D., Juzsakova, T., Viktor, S., Van, S.B., Le, P.-C., Duong La, D., Woong Chang, S., Um, M.-J., Ngo, H.H. and Nguyen, D. (2023). Recent advances and applicable flexibility potential of electrochemical processes for wastewater treatment. Science of

The Total Environment, 867, 161361. https://doi.org/10.1016/j.scitotenv.2022.161361

5. Almukdad, A., Hawari, H.A. and Hafiz, M.A. An enhanced electrocoagulation process for the removal of fe and mn from municipal wastewater using Dielectrophoresis (DEP). Water, 13(4), 485. https://doi.org/10.3390/w13040485
6. Al-Qodah, Z., Tawalbeh, M., Al-Shannag, M., Al-Anber, Z. and Bani-Melhem, K. (2020). Combined electrocoagulation processes as a novel approach for enhanced pollutants removal: A state-of-the-art review. Science of The Total Environment, 744, 140806. https://doi.org/10.1016/j.scitotenv.2020.140806
7. Al-Qodah, Z., Al-Shannag, M., Hudaib, B., Bani-Salameh, W., Shawaqfeh, A.T. and Assirey, E. (2025). Synergy and enhanced performance of combined continuous treatment processes of pre-chemical coagulation (CC), solar-powered electrocoagulation (SAEC), and post-adsorption for Dairy wastewater. Case Studies in Chemical and Environmental Engineering, 11, 101183. https://doi.org/10.1016/j.cscee.2025.101183
8. Al-Shati, M. A., Al-Qodah, Z. and Al-Shannag, M. (2023). Electrocoagulation treatment of high-strength organic wastewater using iron electrodes: Process performance and optimization. Environmental Engineering Research, 28(4), 220231. https://doi.org/10.4491/eer.2022.231
9. Ardianto, R., Samudro, G., Mangkoedihardjo, S. and Izmi, S.T.I. (2025). Integrated approach to textile wastewater treatment: Investigating electrocoagulation, MBBR, and adsorption synergy. Journal of Water Process Engineering, 77, 108364. https://doi.org/10.1016/j.jwpe.2025.108364
10. Aryanti, P.T.P., Nugroho, F.A., Prabowo, B.H., Prasetyo, T., Rahayu, F.S., Kadier, A. and Sher, F. (2022). Integrated electrocoagulation-tight ultrafiltration for river water decontamination: The influence of electrode configuration and operating pressure. Cleaner Engineering and Technology, 9, 100524. https://doi.org/10.1016/j.clet.2022.100524
11. Asaithambi, P., Desta, W.M., Yesuf, M.B., Hussen, M., Asmelash, Z., Beyene, D., Periyasamy, S. and Alemayehu, E. (2024). Photo-alternating current-electrocoagulation technique: Studies on operating parameters for treatment of industrial wastewater. Scientific African, 24, e02193. https://doi.org/10.1016/j.sciaf.2024.e02193
12. Aziz, A.R.A., Asaithambi, P. and Ashri Bin Wan Daud, W.M. (2016). Combination of electrocoagulation with advanced oxidation processes for the treatment of distillery industrial effluent. Process Safety and Environmental Protection, 99, 227–235. https://doi.org/10.1016/j.psep.2015.11.010
13. Bagastyo, A.Y., Nurhayati, E., Manah, S.PH., Iswari, A.A.W.R., Yulikasari, A., Warmadewanthi, I.D.A.A. and Lin, T.F. (2023). The role of aeration and pre-chlorination prior to coagulation-flocculation process in water treatment: A laboratory and field research in Indonesia. Case Studies in Chemical and Environmental Engineering, 7, 100352. https://doi.org/10.1016/j.cscee.2023.100352
14. Bakry, S.A., Matta, M.E., Noureldin, A.M. and Zaher, K. (2024). Performance evaluation of electrocoagulation process for removal of heavy metals from wastewater using aluminum electrodes under variable operating conditions. Desalination and water treatment, 318, 100396. https://doi.org/10.1016/j.dwt.2024.100396
15. Behera, U.S., Poddar, S. and Byun, H-S. (2025). Electrocoagulation treatment of wastewater collected from Haldia industrial region: Performance evaluation and comparison of process optimization. Water Research, 268, Part B, 122716. https://doi.org/10.1016/j.watres.2024.122716
16. Bener, S., Bulca, O., Palas, B., Tekin, G., Atalay, S. and Gülin Ersöz, G. (2019). Electrocoagulation process for the treatment of real textile wastewater: Effect of operative conditions on the organic carbon removal and kinetic study. Process Safety and Environmental Protection, 129, 47–54. https://doi.org/10.1016/j.psep.2019.06.010
17. Bhagawati, P.B., Al Jaberi, F.Y., Ahmed, S.A., Kadier, A., Alwan, H.H., Ajjam, S.K., Shivayogimath, C.B and Babu, B.R. (2022). Electrocoagulation technology for wastewater treatment: Mechanism and applications. In book: Advanced Oxidation Processes in Dye-Containing Wastewater, Ed.1(13), Springer, Singapore. https://doi.org/10.1007/978-981-19-0987-0_13
18. Bhagawati, P.B., Kumar, K.H.S., Lokeshappa, B., Malekdar, F., Sapate, S., Adeogun, A.I., Chapi, S., Goswami, L., Mirkhalafi, S. and Sillanpää, M. (2024). Prediction of electrocoagulation treatment of tannery wastewater using multiple linear regression based ANN: Comparative study on plane and punched electrodes. Desalination and Water Treatment, 319, 100530. https://doi.org/10.1016/j.dwt.2024.100530
19. Bidu, J.M., Van der Bruggen, B., Rwiza, M.J and Njau, K.N. (2021). Current status of textile wastewater management practices and effluent characteristics in Tanzania. Water, Science, & Technology, 83(10), 2363–2376. https://doi.org/10.2166/wst.2021.133
20. Channa, N., Gadhi, T. A., Mahar, R. B., Ali, I., Sajjad, S., Freyria, F. S., Bonelli, B., Widderich, S. and Frechen, F.-B. (2024). Efficient and rapid combined electrocoagulation–filtration of arsenic in drinking water. Water, 16(12), 1684. https://doi.org/10.3390/w16121684

21. De Maman R., da Luz V.C., Behling, L., Dervanoski, A., Dalla Rosa, C. and Pasquali, G.D.L. (2022). Electrocoagulation applied for textile wastewater oxidation using iron slag as electrodes. Environmental Science and Pollution Research, 29(21), 31713–31722. https://doi.org/10.1007/s11356-021-18456-5
22. Fadzli, J., Puasaa, S.W., Hima, N.R.N, Hamida, H.K. and Amri, N. (2024). Electrocoagulation: Removing colour and COD from simulated and actual batik wastewater. Desalination and Water Treatment, 320, 100658. https://doi.org/10.1016/j.dwt.2024.100658
23. Fan, Y., Tegladza, I.D., Zhang, G., Dai, H., Liao, B. and Lu, J. (2023). The in-situ and ex-situ adsorption of iron flocs generated by electrocoagulation: Application for nickel, fluoride and methyl orange removal. Journal of Water Process Engineering, 57, 104586. https://doi.org/10.1016/j.jwpe.2022.103395
24. García-Ávila, F., García-Uzca,C., Quizhpilema-Marín, S., Salazar-Armijos, M.J., Segura-Paima, M. and Valdiviezo-Gonzales, L. (2025). Electrocoagulation for industrial wastewater remediation: efficiency, operational optimization and sustainable implementation: Review paper. Journal of Electrochemical Science and Engineering, 16, 3068. https://doi.org/10.5599/jese.3068
25. Gasmi, A., Elboughdiri, N., Ghernaout, D., Ahmed Hannachi, K.S., Halim, A. and Khan, M.I. (2022). Electrocoagulation process for removing dyes and chemical oxygen demand from wastewater: operational conditions and economic assessment – A review. Desalination and Water Treatment, 271, 74-107. https://doi.org/10.5004/dwt.2022.28792
26. Ghaderi, D. and Rahbani, M. (2021). Tracing suspended matter in Tiab estuary applying ANN and Remote sensing. Regional Studies in Marine Science, 44, 101788. https://doi.org/10.1016/j.rsma.2021.101788
27. Gunawan, A.A., Bloemer, J., Van Riel, A.C.R, and Essers, C. (2022). Institutional Barriers and Facilitators of Sustainability for Indonesian Batik SMEs: A Policy Agenda. Sustainability, 14(14), 8772. https://doi.org/10.3390/su14148772
28. Hashem, S.A.M., Gaber, G.A., Hussein, W.A. and Ahmed, A.S.I. (2024). Electrocoagulation process with Fe/Al electrodes to eliminate pollutants from real and synthetic wastewater. Results in Materials, 23, 100606. https://doi.org/10.1016/j.rinma.2024.100606
29. Hellal, M.S., Doma, H.S. and Abou-Taleb, E.M. (2023). Techno-economic evaluation of electrocoagulation for cattle slaughterhouse wastewater treatment using aluminum electrodes in batch and continuous experiment. Sustainable Environment Research, 33, 2. https://doi.org/10.1186/s42834-023-00163-0
30. Islam, M.M., Aidid, A.R., Mohshin, J.N., Mondal, H., Ganguli, S. and Chakraborty, A.K. (2025). A critical review on textile dye-containing wastewater: Ecotoxicity, health risks, and remediation strategies for environmental safety. Cleaner Chemical Engineering, 11, 10065. https://doi.org/10.1016/j.clce.2025.100165
31. Issaka. E. (2024). From complex molecules to harmless byproducts: Electrocoagulation process for water contaminants degradation. Desalination and Water Treatment, 319, 100532. https://doi.org/10.1016/j.dwt.2024.100532
32. Jing, G., Zhou, M., Wang, X. and Wu, Z. (2020). Removal of organic pollutants from wastewater by electrocoagulation using iron electrodes: Mechanism and performance evaluation. Water, 12(2), 595. https://doi.org/10.3390/w12020595
33. Kholisoh, S., Wulandari, I., Iryani, A., Latif, S. and Wanarsih, S. (2022). Characterization of batik industrial wastewater in Bogor City. HELIUM: Journal of Science and Apllied Chemistry, 2(1), 20-24. https://journal.unpak.ac.id/index.php/he_jsac
34. Kusumawardani, S.D.A., Kurnania, T.B.A., Astarib, A.J., and Sunardi. (2024). Readiness in implementing green industry standard for SMEs: Case of Indonesia's batik industry. Heliyon, 10(16), e36045. https://doi.org/10.1016/j.heliyon.2024.e36045
35. Lamhar, R., Kambuyi, T.N., Bejjany, B., Kherbeche, A., Digua, K. and Adil Dani, A. (2024). Electrocoagulation for the decolorization of textile wastewater in single-channel reactor: Response surface methodology for optimization and a novel model exploitation. Journal of Cleaner Production, 450, 141900. https://doi.org/10.1016/j.jclepro.2024.141900
36. Manikandan, S. and Saraswathi, R. (2023). Electrocoagulation-based treatment of textile wastewater using iron electrodes: Influence of operating parameters and energy consumption. Journal of Environmental Chemical Engineering, 11(2), 109301. https://doi.org/10.1016/j.jece.2023.109301
37. Phang, F. A., Roslan, A. N., Zakaria, Z. A., Zaini, M. A. A., Pusppanathan, J. and Talib, C. A. (2022). Environmental awareness in batik making process. Sustainability, 14(10), 6094. https://doi.org/10.3390/su14106094
38. Phu, T.K.C., Nguyen, P.L. and Phung, T.V.B. (2025). Recent progress in highly effective electrocoagulation-coupled systems for advanced wastewater treatment. iScience, 28(3), 111965. https://doi.org/10.1016/j.isci.2025.111965
39. Rahmadyanti, E. and Febriyanti, C.P. (2020). Feasibility of constructed wetland using coagulation flocculation technology in batik wastewater treatment. Journal of Ecological Engineering, 21(6), 67–77. https://doi.org/10.12911/22998993/123253
40. Rahmadyanti, E. and Wiyono, A. (2020). Constructed

wetland with rice husk substrate as phytotechnology treatment for sustainable batik industry in Indonesia. Journal of Physics: Conference Series, 1569, 042018. https://doi.org/10.1088/1742-6596/1569/4/042018

41. Rahmadyanti, E. and Audina, O. (2020). The performance of hybrid constructed wetland system for treating the batik wastewater. Journal of Ecological Engineering, 21(3), 94–103. https://doi.org/10.12911/22998993/118292
42. Rakhmania, Kamyab, H., Yuzir, M.A., Abdullah, N., Quan, L.M., Riyadi, F.A. and Marzouki, R. (2022). Recent applications of the electrocoagulation process on agro-based industrial wastewater: A review. Sustainability, 14(4), 1985. https://doi.org/10.3390/su14041985
43. Raya, A.B., Andiani, R., Siregar, A.P., Prasada, I.Y., Indana, F., Simbolon, T.G.Y, Kinasih, A.T., and Dwi Nugroho, A.D. (2021). Challenges, Open Innovation, and Engagement Theory at Craft SMEs: Evidence from Indonesian Batik. Journal of Open Innovation: Technology, Market, and Complexity, 7(2), June. https://doi.org/10.3390/joitmc7020121
44. Reátegui-Romero, W., Morales-Quevedoa, S.E., Huanca-Colosa, K.W., Figueroa-Gómez, N.M., King-Santosa, M.E., Zaldivar-Alvarez, W.F., Flores-Del Pinob, L.V., Yuli-Posadasc, R.A., Bulege-Gutiérrez, W. (2020). Effect of current density on COD removal efficiency for wastewater using the electrocoagulation process. Desalination and Water Treatment, 184, 15–29. https://doi.org/10.5004/dwt.2020.25341
45. Reza, A. and Haller, S. (2024). Electrocoagulation as a remedial approach for phosphorus removal from onsite wastewater: A Review. Water, 16(22), 3206, 1–26 https://doi.org/10.3390/w16223206
46. Sadaf, S., Roy, H., Fariha, A., Rahman, T.U., Tasnim, N., Jahan, N., Sokan-Adeaga, A.A., Safwat, S.M. and Islam, M.S. (2024). Electrocoagulation-based wastewater treatment process and significance of anode materials for the overall improvement of the process: A critical review. Journal of Water Process Engineering, 62, 105409. https://doi.org/10.1016/j.jwpe.2024.105409
47. Salinas-Echeverría, D.D., Sánchez-De La Cruz, L.C, Zambrano-Intriago, L.A., Rodríguez-Díaz, J.M., Sanoja-Lopez, K.A., Luque, R., Fernández-Andrade, K.J., Yunet Gómez-Salcedo, Y. and Baquerizo-Crespo, R.J. (2023). Chemical Engineering Research and Design, 198, 478–488. https://doi.org/10.1016/j.cherd.2023.08.049
48. Shah, A.A., Walia, S. and Kazemian. (2024). Advancements in combined electrocoagulation processes for sustainable wastewater treatment: A comprehensive review of mechanisms, performance, and emerging applications. Water Research, 252(15), March, 121248. https://doi.org/10.1016/j.watres.2024.121248
49. Susilowati, S., Sutrisno, J., Masykuri, M. and Maridi, M. (2018). Dynamics and factors that affects DO-BOD concentrations of Madiun River. AIP Conference Proceeding. 2049, 020052. https://doi.org/10.1063/1.5082457
50. Tabash, I., Elnakar, H. and Khan, M.F. (2024). Optimization of iron electrocoagulation parameters for enhanced turbidity and chemical oxygen demand removal from laundry greywater. Scientific Reports, 14, 16468. https://doi.org/10.1038/s41598-024-67425-8
51. Tangahu, B.V., Ningsih, D.A., Kurniawan, S.B., and Imron, M.F. (2019). Study of BOD and COD removal in batik wastewater using Scirpus grossus and Iris pseudacorus with intermittent exposure system. Journal of Ecological Engineering, 20(5), 130–134. https://doi.org/10.12911/22998993/105357
52. Tegladza, I.D., Xu, Q., Xu, K., Guojun L.V. and Lu, J. (2021). Electrocoagulation processes: A general review about role of electro-generated flocs in pollutant removal. Process Safety and Environmental Protection, 146, 169–189. https://doi.org/10.1016/j.psep.2020.08.048
53. Triwiswara, M. (2019). Efficiency assessment of batik industry wastewater treatment plant in center for handicraft and batik Indonesia. Advances in Engineering Research, 187. Third International Conference on Sustainable Innovation 2019 – Technology and Engineering (IcoSITE 2019). https://doi.org/10.2991/icosite-19.2019.23
54. Wang, X., Jiang, J. and Gao, W. (2022). Reviewing textile wastewater produced by industries: characteristics, environmental impacts, and treatment strategies. Water Science Technology, 85(7), 2076–2096. https://doi.org/10.2166/wst.2022.088
55. Worku, A.K., Ayele, D.W., Teshager, M.A., Omar, M., Yerkrang, P.P., Elgaddafi, R. and Alemu, M.A. (2025). Recent advances in wastewater treatment technologies: Innovations and new insights. Energy Reviews, 4, 100164. https://doi.org/10.1016/j.enrev.2025.100164
56. Xie, F., Gao, C. and Avérous, L. (2024). Alginate-based materials: Enhancing properties through multiphase formulation design and processing innovation. Materials Science and Engineering, 159, 100799. https://doi.org/10.1016/j.mser.2024.100799
57. Zakaria, N., Rohani, R., Mohtar, W.H.M.W., Purwadi, R., Sumampouw, G.A., and Indarto, A. (2023). Batik effluent treatment and decolorization—A review. Water, 15, 1339. https://doi.org/10.3390/w15071339